Electronic transport calculations for self-assembled monolayers of 1,4-phenylene diisocyanide on Au(111) contacts

Robert Dahlke and Ulrich Schollwöck

Sektion Physik and Center for Nanoscience, LMU München, Theresienstrasse 37, D-80333 München, Germany
(Received 8 October 2003; published 27 February 2004)

We report on electronic transport calculations for self-assembled monolayers of 1,4-phenylene diisocyanide on Au(111) contacts. Experimentally one observes more structure (i.e., peaks) within the measured conductance curve for this molecule with two isocyanide groups, compared to measurements with molecules having thiol groups. The calculations are performed on the semiempiric extended Hückel level using elastic scattering quantum chemistry, and we investigate three possible explanations for the experimental findings. Comparing the experimental and theoretical data, we are able to rule out all but one of the scenarios. The observed additional peaks are found to be only reproduced by a monolayer with additional molecules perturbing the periodicity. It is conjectured that the weaker coupling to Au of isocyanide groups compared to thiol groups might be responsible for such perturbations.

I. INTRODUCTION

Within the last decade an increasing interest in molecular electronics has developed, with the expectation of realizing molecular diodes and transistors. This is based on the progress in manipulation techniques, which now allow the controlled attachment of atomic scale structures like molecules to mesoscopic leads. With these new devices one is able to determine the conductance properties of molecular structures. Explaining and predicting the electronic behavior of such devices is an essential step towards their design and use as nanoscale electronic circuits.

To this end a number of theoretical studies have been performed with the aim of reproducing measured *IV* characteristics. These studies differ in the way they take the electronic levels of the molecules, their modification by the coupling to the leads, and the change of electrostatic potential due to bias into account. Semiempiric methods[1−3] have been used, as well as first principles techniques,[4−7] the latter being restricted to systems of moderate size.

The wide range of experimentally observed behavior (see Sec. II) suggests that not only the structure of the molecule, but also the details of the device fabrication, affect the conduction properties of molecular devices. The crucial step is the deposition of molecules onto the surface of the lead. As this is achieved by self-assembly the amount of adsorbed molecules and their individual positions cannot be exactly controlled and therefore remains unknown. A satisfactory understanding of the interplay between geometrical alignment of the molecules and measured conductance properties has thus not yet been achieved (for a recent review, see, e.g., Ref. 8).

In this paper we study the way in which changing the geometrical alignment of the monolayer has an influence on the conduction properties of a molecular device. In so doing we can rule out a number of explanations which have previously been considered[9] to explain the occurrence of additional structure in the conductance-voltage (*CV*) characteristics.

The outline is the following: first we summarize some of the recent experimental findings. Then the method we use (based on elastic scattering quantum chemistry[10]) for calculating the conductance properties of molecular devices, is discussed. Calculations for the conductance of a self-assembled monolayer, being built of 1,4-phenylene diisocyanide (PDI) and sandwiched between gold leads are then presented. The results for three qualitatively different geometrical constitutions of the mono-layer are compared with experimental data. By this we can rule out all but one and conclude that the only geometrical alignment, which gives rise to several peaks in the conductance curve, is a mono-layer with additional molecules perturbing the periodicity.

II. EXPERIMENTAL OVERVIEW

The devices built to study conductance properties of molecular structures differ not only in amount and chemical structure of the molecules in use but also in the way these are attached to metallic or semiconducting leads. Single or few molecules are accessible in mechanically controllable break junctions (MCBs) and with the scanning tunneling microscope (STM). Many molecules are involved in sandwiched self-assembled monolayer (SAM) experiments. The observed properties depend on the exact geometry of the device. The conductance differs in orders of magnitude and the qualitative voltage dependency of the current ranges from simple ohmic behavior to negative differential resistance.[11]

In the past Reed *et al.*[12] have measured the electrical conductance of a self-assembled molecular monolayer bridging a MCB at room temperature. Molecules of 1,4-benzene dithiol (i.e., having two thiol groups, which are known to couple strongly to Au atoms) were used and the *CV* characteristic was found to be symmetric with one peak in the voltage range of 0–2V. They measured a current of the order

FIG. 1. Molecular structure of 1,4-phenylene diisocyanide.

of 50 nA at a bias voltage of 2 V, which they claim is produced by transport through one single active molecule. Reichert *et al.*[13] also used a MCB with molecules having two thiol groups, but being considerably longer. The measured current amplitude was about 500 nA at 1 V, i.e. although the molecule was more than twice as long, the current was ten times larger.

With a different setup, where a SAM is sandwiched between two metallic leads, Chen *et al.*[11] have found negative differential resistance, namely one peak at 2V in the *IV* curve. The molecule under investigation had one thiol group only and was attached to Au leads at both ends. The measurements were taken at room temperature and the measured current maximum was of the order of 1nA.

Only recently, sandwiched SAM devices at 4.2 K were studied,[9,14] where a benzene ring with two isocyanide instead of thiol groups was used (see Fig. 1). The measurements exhibited currents of the order of 50–400 nA. The *CV* characteristic for this molecule revealed more structure, in form of three to five peaks within a voltage range of 1 V. Such a behavior was not observed with previous devices containing other molecules.

III. THEORETICAL FORMALISM

In the literature there has been presented quite a number of techniques to calculate nonequilibrium electronic transport through molecular systems attached to mesoscopic leads. Usually the Landauer formalism is applied, which describes current as elastic electron transmission and therefore requires the transmission function $T(E)$. To this end one needs a framework that allows for a description of the molecular device on the atomic level. This involves not only the molecules themselves, but also the surface and bulk region of the leads. Quantum chemistry provides such a framework, and one can choose the level of theory according to the size of the system under consideration and the computational effort one is willing to spend.

Using a quantum chemistry method, the transmission function can be obtained from an effective one-particle Hamiltonian, which is an appropriate description for strong coupling of the molecules to the leads (as in the case of covalent binding). The methods differ in the generation of the one-particle Hamiltonian, which might be based on semi-empirical grounds[1–3] or on first-principles and self-consistent techniques.[4–7]

A different approach,[15] taking many-particle effects explicitly into account, uses a master equation with transition rates calculated perturbatively using the golden rule. This approach is appropriate for weak coupling.

We use the Landauer formalism, as the molecules are assumed to be chemically bonded to the gold contacts (i.e., strong coupling), together with the semiempiric extended
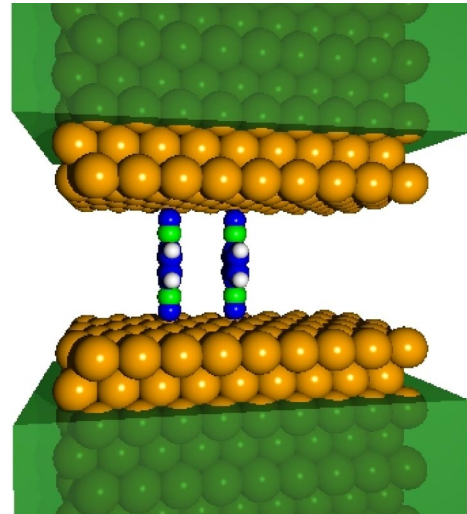
FIG. 2. (Color online) Partitioning of the system into three parts: the two semi-infinite leads $\Sigma_{1,2}$ (surrounded by boxes) and the molecular region Σ_0 between them.

Hückel elastic scattering quantum-chemistry (ESQC) method.[10] The molecular structure is optimized[16] beforehand. This approach, though limited as compared to more sophisticated quantum chemistry methods, is yet justified because we want to gain a qualitative understanding of a many molecule experiment which cannot be described by first-principle techniques, as the number of atoms involved is beyond the practical limitations of to-date computer resources.

A. Landauer formalism

According to the Landauer formula, current along a defect region is the result of electron transmission from the source to the drain lead, described by the transmission function $T(E)$. For chemical potentials μ_1 and μ_2 of source and drain lead, shifted with respect to each other by an applied voltage $\mu_1 = \mu_2 + eV$, the current reads

$$I = \frac{-2e}{h} \int_{-\infty}^{\infty} T(E)[f(E-\mu_1) - f(E-\mu_2)]dE, \quad (1)$$

where $f(E)$ is the Fermi function. The Landauer formula is valid under the condition that transport is coherent across the molecule, which is plausible as the typical mean free path of electrons within metals is of the order of 500 nm, while the molecular gap between source and drain lead is only about 1–5 nm in length.

The system is formally partitioned into three regions $\Sigma_i, i \in \{0,1,2\}$, two of them ($\Sigma_{1,2}$) containing the semi-infinite leads, the third one (Σ_0) being the finite region containing all molecules as well as a few surface layers of each lead (see Fig. 2). We use periodic boundary conditions in the directions perpendicular to the surface normal.

By a tight binding approximation, the infinite-dimensional Hamiltonian of the entire system can be composed of quantum chemical one-particle block Hamiltonians of finite dimension:

$$H = \sum_{i \in \text{mol}} \left(\varepsilon_i c_{mi}^\dagger c_{mi} + \sum_{j \neq i} H_{ij}^m c_{mi}^\dagger c_{mj} \right)$$

$$+ \sum_{d \in \text{leads}} \sum_{l=l_0}^{\infty} \sum_{i \in l} \left(\varepsilon_{dli} c_{dli}^\dagger c_{dli} + \sum_{j \neq i} H_{llij}^d c_{dli}^\dagger c_{dlj} \right)$$

$$+ \sum_{d \in \text{leads}} \sum_{l=l_0}^{\infty} \sum_{\substack{i \in l \\ j \in l+1}} (H_{l,l+1,ij}^d c_{dli}^\dagger c_{d,l+1,j} + \text{H.c.})$$

$$+ \sum_{d \in \text{leads}} \sum_{i \in l_0} \sum_{j \in \text{mol}} (H_{l_0 ij}^{dm} c_{dl_0 i}^\dagger c_{mj} + \text{H.c.}). \qquad (2)$$

The first summation describes the isolated molecular region, by an on-site energy ε and a hopping term. The indices i and j run over the orbital basis set within that region. The next two summations describe the isolated leads, labeled by d. Layer by layer, starting with the surface layer l_0, the first term accounts for intra-layer interactions, while the second one describes the interaction between layers. Finally the last term describes the coupling between the molecular region and each lead. Note that only the first layer l_0 contributes to that term and that there is no interaction between different leads. These are only formal restrictions, as parts of each lead can be included into the molecular region.

The determination of the transmission function involves two steps. First the conduction properties of the isolated leads have to be calculated. Thereby each lead will be decomposed into conducting and nonconducting incoming and outgoing channels. These correspond to propagating and evanescent solutions moving in one of two possible directions, respectively. In a second step, the channels are connected to each other via the molecular region. This is described by the scattering matrix and the transmission function is finally obtained by summing up the contribution from each channel.

The calculation can be performed either using Green's function techniques[17] or equivalently[18] using ESQC,[10,19] which is a scattering-matrix approach. We present the details of the calculation in the second scheme, as individual contributions from each channel to the transmission function can then be easily studied.

B. Bulk propagator

First we will restrict our attention to the semi-infinite lead Hamiltonians, which do not have to be identical. The Hamiltonians of Eq. (2) for one lead d, namely, $H_{ll'}^d$, are layer independent, if one assumes periodicity, i.e., $H_{ll}^d = H_{l_0 l_0}^d$ and $H_{l,l+1}^d = H_{l_0,l_0+1}^d$. Using Bloch's theorem one can reduce the infinite dimensional system of equations to an $N \times N$-matrix equation (N being the number of orbital basis functions in one layer)

$$[M_d(E) + h_d(E)e^{ik\Delta} + h_d^\dagger(E)e^{-ik\Delta}] \gamma_l(k,E) = 0, \quad \forall l, \qquad (3)$$

with $M_d(E) := H_{l_0 l_0}^d - ES_{l_0 l_0}^d$, $h_d(E) := H_{l_0,l_0+1}^d - ES_{l_0,l_0+1}^d$, and $S_{ll'}^d$ is the overlap matrix between orbitals in layer l and layer l' of lead d for cases when one does not deal with an orthonormal basis set (otherwise $S_{ll'}^d = \text{Id} \cdot \delta_{ll'}$). With Δ we denote the lattice spacing and the layer coefficients γ_l obey the relation $\gamma_{l+1} = e^{ik\Delta} \gamma_l$. Defining $\lambda := e^{ik\Delta}$ one can easily see that Eq. (3) is an $N \times N$ quadratic eigenvalue equation. It can be transformed into a $2N \times 2N$ linear eigenvalue problem:

$$P_d(E) \begin{pmatrix} \gamma_l \\ \gamma_{l+1} \end{pmatrix} = \lambda \begin{pmatrix} \gamma_l \\ \gamma_{l+1} \end{pmatrix}, \qquad (4)$$

$$P_d(E) := \begin{bmatrix} 0 & 1 \\ -h_d^{-1} h_d^\dagger & -h_d^{-1} M_d \end{bmatrix} \qquad (5)$$

(where we have dropped the energy- and k-dependency of γ_l for notational ease). This layer-to-layer propagator $P_d(E)$ also connects the coefficients of adjacent layers

$$\begin{pmatrix} \gamma_l \\ \gamma_{l+1} \end{pmatrix} = P_d(E) \begin{pmatrix} \gamma_{l-1} \\ \gamma_l \end{pmatrix} \qquad (6)$$

and therefore reduces the problem of finding solutions for the entire isolated lead Hamiltonian to specifying the wave function coefficients at two adjacent layers γ_l and γ_{l+1} only.

All possible solutions at energy E can be decomposed into independent channels, by solving for the eigenvalues of Eq. (4). These eigenvalues come in pairs such that for each eigenvalue $\lambda_>$, there exists a corresponding eigenvalue $\lambda_<$ satisfying the relation $\lambda_> = 1/\lambda_<^*$, as can be seen by transposing Eq. (3). Eigenvalues with $|\lambda| \neq 1$, i.e., complex k, belong to exponentially diverging solutions [see Eqs. (6) and (4)]. These are of course non physical, as long as the lead is infinite. In semi-infinite leads however (which we are dealing with), exponentially decaying coefficients at the boundary will contribute to the surface wave function and must not be neglected.

C. Current operator

The contribution from a single channel to the net current cannot directly be seen from Eq. (4). It depends on the current density associated with a solution to the Schrödinger equation $i\hbar \partial_t S\gamma = H\gamma$ and is obtained via the continuity equation. The probability amplitude $|\gamma|^2$ for a stationary solution is constant in time,

$$\frac{\partial}{\partial t} \gamma^\dagger S \gamma = \frac{i}{\hbar} [\gamma^\dagger H \gamma - \gamma^\dagger H^\dagger \gamma] = 0, \qquad (7)$$

because H and S are hermitian. For the probability amplitude at all layers between l_1 and l_2 one therefore has

$$0 = \frac{\partial}{\partial t} \sum_{l=l_1}^{l_2} (\gamma_l^\dagger S \gamma_l) = \frac{i}{\hbar} \sum_{l=l_1}^{l_2} \gamma_l^\dagger (H - H) \gamma_l$$

$$= \frac{i}{\hbar} [\gamma_{l_1-1}^\dagger h(E) \gamma_{l_1} + \gamma_{l_1+1}^\dagger h^\dagger(E) \gamma_{l_1} - \text{H.c.}]$$

$$+ \frac{i}{\hbar} [\gamma_{l_2-1}^\dagger h(E) \gamma_{l_2} + \gamma_{l_2+1}^\dagger h^\dagger(E) \gamma_{l_2} - \text{H.c.}]$$

$$= \langle \gamma | l_2, l_2+1 \rangle \frac{i}{\hbar} \begin{bmatrix} 0 & -h \\ h^\dagger & 0 \end{bmatrix} \langle l_2, l_2+1 | \gamma \rangle$$

$$- \langle \gamma | l_1-1, l_1 \rangle \frac{i}{\hbar} \begin{bmatrix} 0 & -h \\ h^\dagger & 0 \end{bmatrix} \langle l_1-1, l_1 | \gamma \rangle, \qquad (8)$$

with the projectors $\langle l | \gamma \rangle := \gamma_l$. This gives rise to the definition of the current operator W_l for layer l as

$$W_l := |l, l+1 \rangle \frac{i}{\hbar} \begin{bmatrix} 0 & -h \\ h^\dagger & 0 \end{bmatrix} \langle l, l+1 |. \qquad (9)$$

Now let both φ and ϑ be solutions at fixed energy E with the eigenvalues λ_1 and λ_2 respectively. Because the expectation value for W_l is layer independent [Eq. (8)] one has

$$\langle \vartheta | W_l | \varphi \rangle = \langle \vartheta | W_{l+1} | \varphi \rangle$$

$$= \lambda_1 \lambda_2^* \langle \vartheta | W_l | \varphi \rangle. \qquad (10)$$

This equation describes the connection between the current properties of a solution φ and its eigenvalue λ. We summarize the results of a detailed analysis of this equation, which is given in Appendix A. Each channel $|\varphi_i \rangle$ can be assigned a current value v_i, defined as

$$v_i := \text{Im} \langle \varphi_i | W | \varphi_i \rangle, \qquad (11)$$

where we have used the layer independence of W_l in simply writing W.

Channels with eigenvalue modulus $|\lambda| \neq 1$, i.e., evanescent waves have zero current value. They therefore do not contribute to the current. (Yet they are important at the surface, as already mentioned above.) Only channels with an eigenvalue of modulus 1 ($|\lambda| = 1$) contribute to the current. The sign of v_i determines the direction of charge transport.

Solutions for an isolated lead are linear combinations of propagating waves in opposite directions, with the same amount of current being transported in each direction, thus carrying no net current, and resulting in a standing wave.

We now define $\Lambda_>$ and $\Lambda_<$ as the two $N \times N$ diagonal matrices composed of all incoming and outgoing eigenvalues $\Lambda_{\gtrless} := \text{diag}(\lambda_{\gtrless}^i)$. The $2N \times 2N$ matrices U and $U^{-1}PU$ have the following forms:

$$U^{-1}PU = \begin{bmatrix} \Lambda_> & 0 \\ 0 & \Lambda_< \end{bmatrix}, \quad U := \begin{bmatrix} U_> & U_< \\ U_> \Lambda_> & U_< \Lambda_< \end{bmatrix}. \qquad (12)$$

D. Scattering matrix

Up to now, we have considered the isolated leads only. These are now assumed to be each coupled to the molecular defect region and thereby indirectly coupled to one another. We are interested in stationary solutions which consist of an incoming propagating wave in one lead, being scattered among all the accessible outgoing channels (propagating and evanescent ones). This information is contained in the scattering matrix $\mathcal{S}$, which is shown in Appendix B to be of the form

$$\mathcal{S} = -M_{\text{in}}^{-1} \cdot M_{\text{out}}. \qquad (13)$$

It is important to notice that the scattering matrix is always quadratic, because in each lead there are the same amount of incoming and outgoing channels and the scattering matrix connects all outgoing channels to all incoming ones. This is opposed to the transfer matrix $\mathcal{T}$, which determines the amplitudes of in- and outgoing waves in the drain lead given the in- and outgoing waves of the source lead. This matrix is quadratic only if both leads have the same number of channels. It then is of the form[20]

$$\mathcal{T} = \begin{bmatrix} F & G^\dagger \\ G & F^\dagger \end{bmatrix}, \qquad (14)$$

and the relation to the scattering matrix is[20]

$$\mathcal{S} = \begin{bmatrix} -F^{\dagger(-1)}G & F^{\dagger(-1)} \\ F^{-1} & G^\dagger F^{\dagger(-1)} \end{bmatrix}. \qquad (15)$$

Methods calculating the scattering matrix via the transfer matrix[19] fail, if two types of leads are used, because F is then no longer quadratic and cannot be inverted. Therefore one commonly takes source and drain lead to be identically constituted. But even in such cases, these methods become numerically unstable, with increasing distance between the molecular region and one lead. This is because the matrix elements of F and G [in Eq. (14)] diverge exponentially, with increasing lead separation. Taking the inverse of F is therefore a numerically critical procedure. Both these problems are avoided by the direct calculation of the scattering matrix, which we present in Appendix B. This calculation is well defined without any restrictions to the number of leads and their composition. Therefore it is not necessary to restrict to identical leads. Furthermore it allows a numerically stable determination of the scattering matrix, even for large lead separations.

E. Transmission function

The transmission function is the sum over the contributions from each combination of incoming channels in the source lead to outgoing channels in the drain lead: $T(E) = \sum_{i,j} T_{j \leftarrow i}$. The relation between the scattering matrix $\mathcal{S}$ and these transmission function elements is

$$T_{j \leftarrow i} = |(\mathcal{S}_{21})_{j \leftarrow i}|^2 \frac{v_j}{v_i}, \qquad (16)$$

where $\mathcal{S}_{21}$ is that block of $\mathcal{S}$ combining the incoming source channels with the outgoing ones in the drain lead. The weighting with velocity factors comes about because the scattering matrix $\mathcal{S}$ does not relate current densities, but wave amplitudes. The current densities are obtained from these wave amplitudes by multiplication with the corresponding velocity factor v_j. The factor v_i in the denominator normalizes the transmission function to be exactly one for perfect transmission. If $v_i = 0$ then $T_{j \leftarrow i} = 0$, because incom-

ing evanescent waves have zero amplitude at the surface. The total current is made up of the contribution from each channel:

$$T(E) = \sum_{i \in \text{source}} \sum_{j \in \text{drain}} T_{j \leftarrow i}(E). \qquad (17)$$

IV. CALCULATIONS FOR PDI

Low temperature experiments with PDI SAMs sandwiched between two metallic leads show several peaks in the CV diagram.[9,14] The typical voltage differences of these peaks are in the range of $\Delta U \approx 0.2$ V (i.e., there are about five peaks within $U = 0$ and 1 V). The commonly adopted explanation for the occurrence of such peaks is the following. Each molecular orbital that enters the energy window, which is opened by the applied voltage, enables resonant tunneling. This increases the conductance and therefore results in a peak within the CV diagram.

Typically, the energy gap between molecular orbitals is in the range of $\Delta E \approx 1$ eV. In other words, for applied voltages up to $U = 1$ V there should be only a single accessible orbital per molecule, giving rise to only a single peak in the CV diagram. Therefore the following question arises: are there geometrical alignments of the molecules such that the additional peaks in the CV diagram can also be explained by resonant tunneling through molecular orbitals?

Influence of changes in the molecular alignment to the transmission spectrum

During the device fabrication, the step under least experimental control is the adsorption of the molecules onto the leads. Therefore the exact geometrical alignment of the molecular SAM and, at least in the sandwich geometry, also the atomic shape of the top metallic lead, is not exactly known. One therefore has to expect not only one specific but rather quite a variety of molecular alignments to be produced. As one is interested in the conduction properties of the resulting device, it is important to understand the influence of each type of geometrical alignment to the transmission function.

To this end, we have investigated three such possible alignments, which will be discussed separately. First we look at the influence of metallic clusters within the contact region between lead and molecule. Then we investigate the difference between single and many molecule experiments and finally we consider the case of molecular clusters.

1. Influence of metallic clusters

In the sandwich geometry, first the bottom metallic lead is created. Then the molecular monolayer is adsorbed on top of it by self-assembly. Finally the top metallic lead is build upon the molecular monolayer. The exact shape of neither metallic surface is known and may be anything but flat and regular. It is likely that the surface atoms of the metallic leads build up clusters [as, for example, in Fig. 3(b)].

The influence of such a Au cluster on the molecular electronic structure is twofold. First it introduces new electronic levels, and second the existing molecular electronic levels
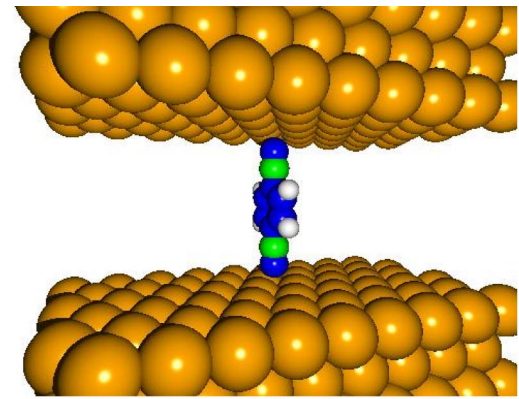
(a)
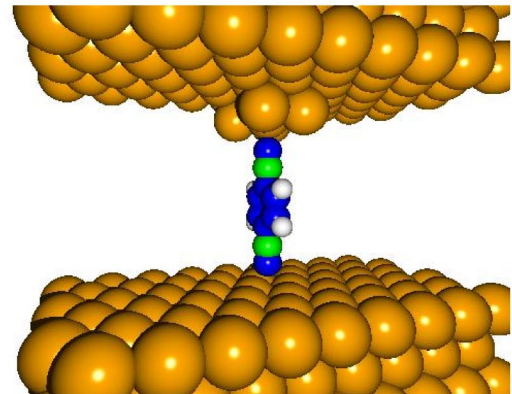
(b)
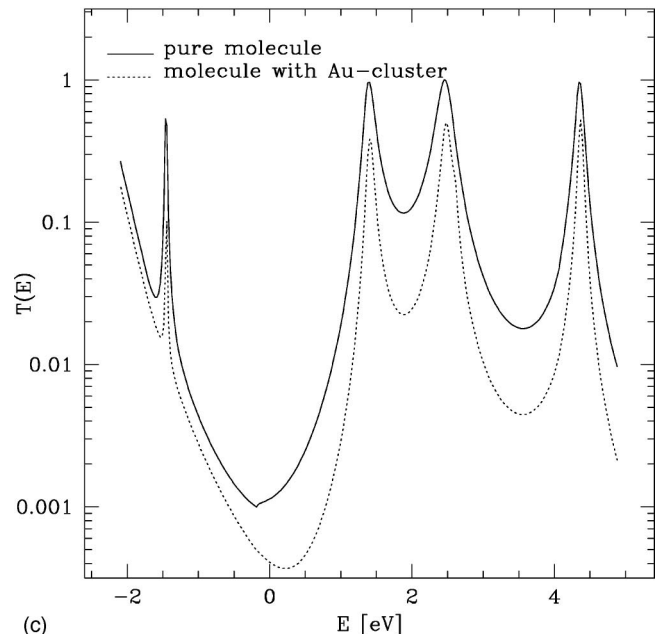
(c)

FIG. 3. (a) (Color online) Structure for a molecule without cluster. (b) (Color online) Structure for a molecule with a gold cluster on top. (c) Transmission function $T(E)$ for both structures. The energy scale is relative to the highest occupied–lowest unoccupied molecular orbital gap, such that $E = 0$ corresponds to the middle of the gap.
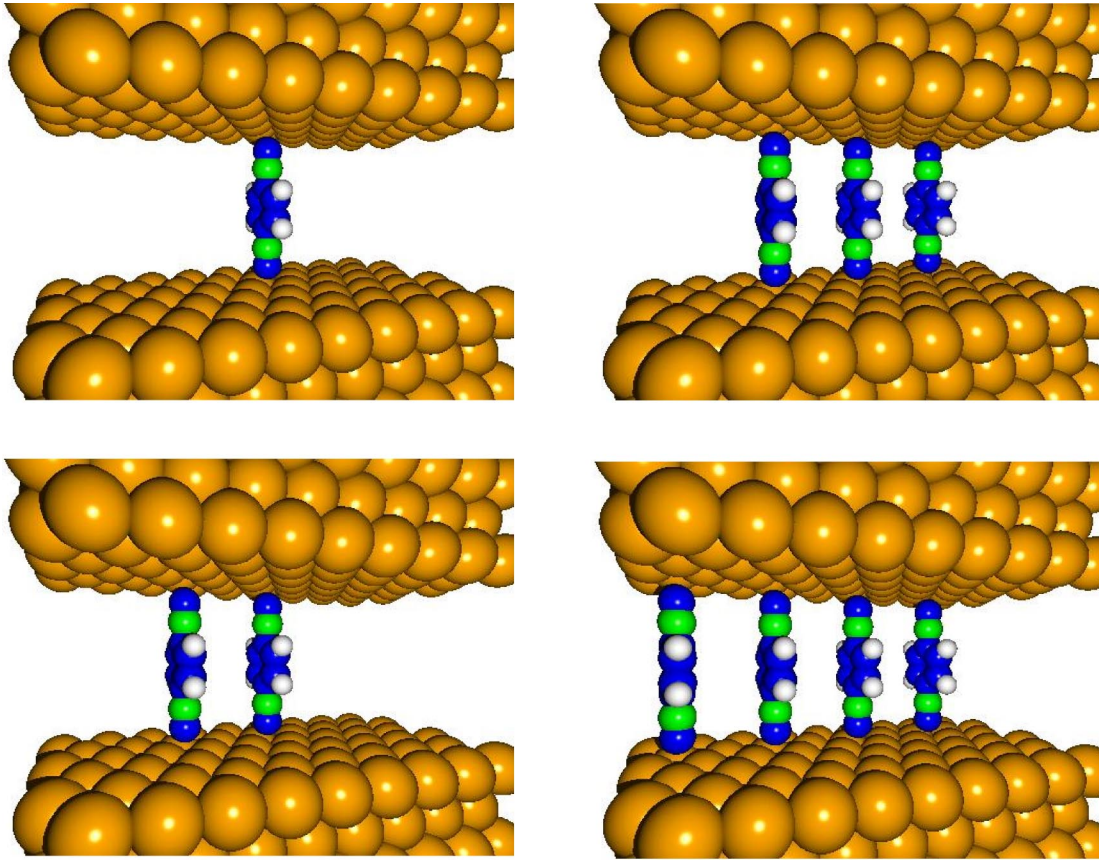
FIG. 4. (Color online) The structure for one, two, three, and four molecules adsorbed within an Au-9×3 supercell. This setup was used to test the sum rule.

will be shifted, by an amount which depends on the strength of the coupling between cluster and molecule. The latter effect will result in a shifted peak in the transmission function, only if the coupling between cluster and molecule is different to the coupling between top electrode and molecule. For clusters similar to the one shown in Fig. 3(b), this is however not the case. The energetic peak positions are identical, as can be seen in Fig. 3(c).

Furthermore, there are no additional peaks, which one might have expected because of the additional electronic levels of the cluster. The explanation for their absence is the following: an electronic level gives rise to a peak in the transmission function only, if the corresponding orbital wave function overlaps with both the top and bottom electrodes. The overlap with the electrode the cluster is attached to (say the top electrode) is of course large. The overlap with the bottom electrode consists of two parts: the direct overlap and the indirect overlap via the molecule. The direct overlap is negligible due to the large spatial separation. The indirect overlap depends on the molecular orbital wave function. If the energy of the cluster level does not coincide with a molecular energy level, then there is no indirect overlap. Only if two levels coincide, the indirect coupling is large, but in that case, there already exists a transmission peak due to the molecule itself.

Therefore if transmission is already suppressed by the molecule (at all off-resonant energies), it can either be fur-

ther reduced by off-resonant tunneling through the cluster, or it can (at best) be left unchanged by resonant tunneling through the cluster. Under no circumstances can transmission, once suppressed by the molecule, be afterwards increased by the cluster. This in turn means that metallic clusters cannot give rise to additional peaks in the transmission spectrum.

2. Monolayer vs single molecule

What do we expect the transmission function $T^i(E)$ for i periodically arranged molecules to look like? As long as the intermolecular interactions are small (compared to the intramolecular ones) the molecular levels of each molecule will not be significantly changed. Furthermore, as the monolayer consists of only one kind of molecule, all of them will have the same electronic structure. Therefore we expect each molecule to contribute the same amount to the transmission function: $T^n(E) := \Sigma_i T^1(E) = n T^1(E)$, where i runs over all n adsorbed molecules.

We calculated the transmission function for $n = 1-4$ molecules within a Au supercell of size 9×3 (the structures are shown in Fig. 4). The distance between the molecules is chosen to be a multiple of the closest Au-Au separation a ($d = 5.76$ Å $= 2a$, with $a = 2.88$ Å). To our knowledge, the parameters of the PDI-SAM monolayer have never been determined experimentally, which is why we have to assume
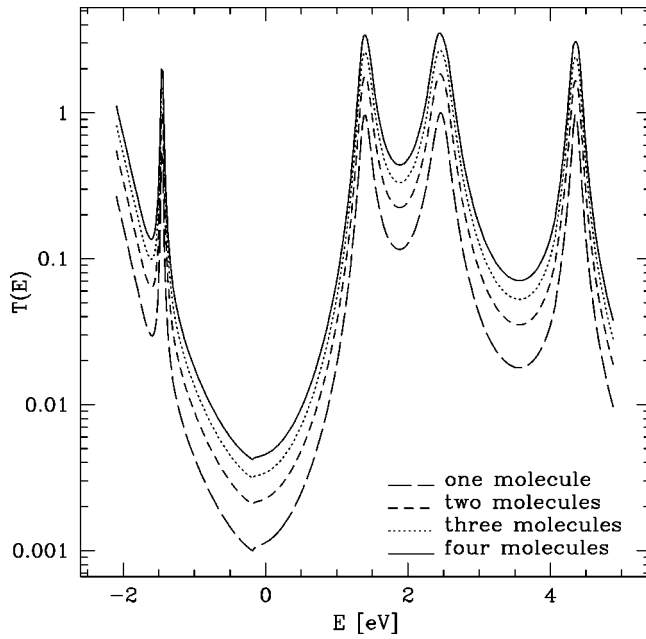
FIG. 5. Transmission function for one, two, three, and four PDI molecules.

the above values. However STM studies[21] and also theoretical calculations[22] have been performed for alkanethiol monolayers, and these parameters motivated our choice.

Independent of the number of molecules present, the transmission functions have the same amount of peaks, at identical energetic positions (see Fig. 5). This result is also obtained for all larger distances of the molecules, where the inter-molecular interaction is even smaller. Furthermore the sum rule is indeed fulfilled, i.e., the calculated transmission functions can well be fitted to the relation $T^n(E) = a(n,m)T^m(E)$, where the deviation of $a(n,m)$ from the theoretically expected value of n/m is below 6% for all $n,m \in \{1,2,3,4\}$. The mere fact that one deals with a monolayer instead of a single molecule does not imply that the transmission function changes qualitatively.

3. Influence of molecular clusters

We now investigate cases where the molecular interactions are not negligible. This occurs for example when the periodic structure of the monolayer is perturbed by an additional molecule, such that a molecular cluster is formed. It is sufficient to study the transmission function of an isolated cluster only, because we have already seen that molecules in the periodic SAM arrangement do not influence each other. The sum of the transmission function for the periodic SAM and the transmission function for the molecular cluster is, due to the sum rule, the total transmission function for the defect and SAM.

We study the influence of a shorter distance between two, three, and four molecules on the transmission spectrum and relate it to the discrete energies of the isolated molecules. The molecules are now separated by $d = 2.88$ Å, which corresponds to the Au-Au atom spacing. The atomic structure for this calculation is shown in Fig. 6(a), the resulting trans-

mission functions in Figs. 6(b) and 6(c).

By reducing the molecular separation the transmission function qualitatively changes. The number of peaks roughly doubles and the new peak positions are different from the ones we obtained in the previous calculations. This time, the peak positions do depend on the number of molecules involved. This is an important point, because if there are several molecular clusters with different molecular distances, then they all give rise to peaks at different energy values. The resulting transmission function is the sum of the individual functions and will thus contain far more peaks than the transmission function for the nonperturbed periodic layer.

The additional peaks are a result of the intermolecular interactions, which split the former degenerate energy levels of the individual molecules, as can be seen in Fig. 7 where we have again plotted the transmission function for three and four molecules, this time together with the discrete energy levels of the corresponding molecular cluster (shown as points along the transmission function) obtained by diagonalizing the molecular Hamiltonian in the absence of all leads. Each of the transmission peaks is related to at least one discrete energy value. But, in turn, not all energy values can be related to a peak in the transmission function, because the corresponding energy level of the molecule does not couple strong enough to the leads.

Finally we show that the additional peak structure in the transmission function for a scenario with an increased intermolecular interaction gives rise to a number of steps in the *IV*-curve. Figure 8 contains an *IV* calculation for a molecular structure containing all three molecular clusters shown in Fig. 6(a). In this calculation the bias voltage V_b enters as a shift of the Fermi levels for source and drain lead: $\mu_1 = \mu_2 + eV_b$. The molecular energy has been set to $E_m = \mu_1 - \delta E_m - \eta eV$, where δE_m is the zero bias displacement of the molecular levels and $\eta = 0.5$, because of the symmetric coupling to the leads.

Compared to the experiments[9,14] the number of steps in the *IV* curve is well reproduced by our calculation. The obtained current is at least one order of magnitude larger than the experimental values.[14] This is a phenomenon common to all theoretical methods based on the Landauer formula.[3,23] A satisfactory explanation for this discrepancy as well as for the broad range of experimentally observed current values has not yet been found.

V. DISCUSSION

We have shown that the peak structure of the transmission function is robust against changes in the number of adsorbed molecules, as long as the distance between molecules is considerably large ($d \gtrsim 6$ Å). And also does the exact shape of the top metallic lead not influence the qualitative structure of the transmission function. Only if the distance between molecules becomes so small that inter-molecular interactions are no longer negligible (which is below 6 Å in our case), does the transmission function undergo a qualitative change. Namely an additional peak structure occurs.

How does this finding compare to the experimental data? As we have pointed out in Sec. II, only in devices using
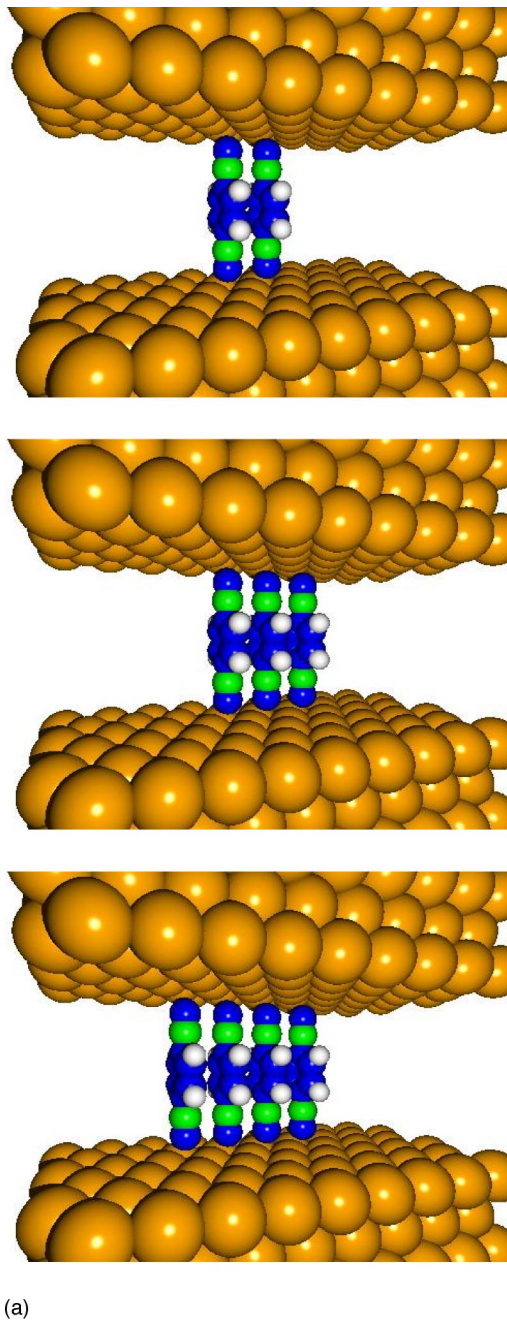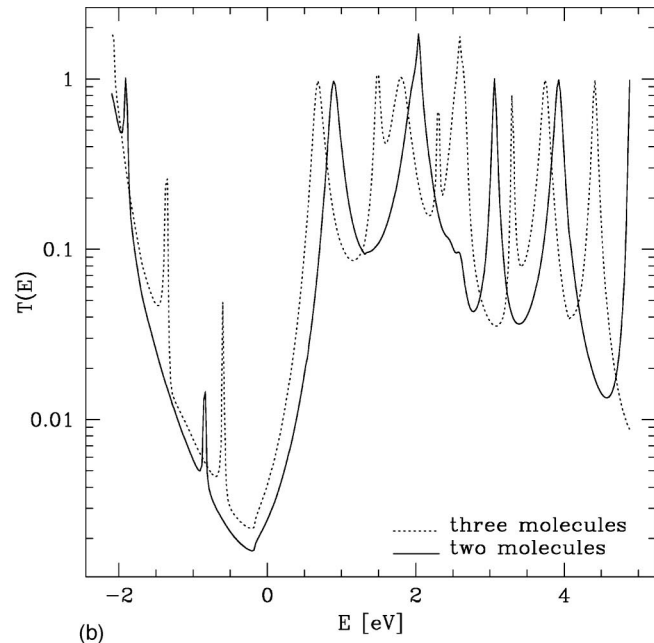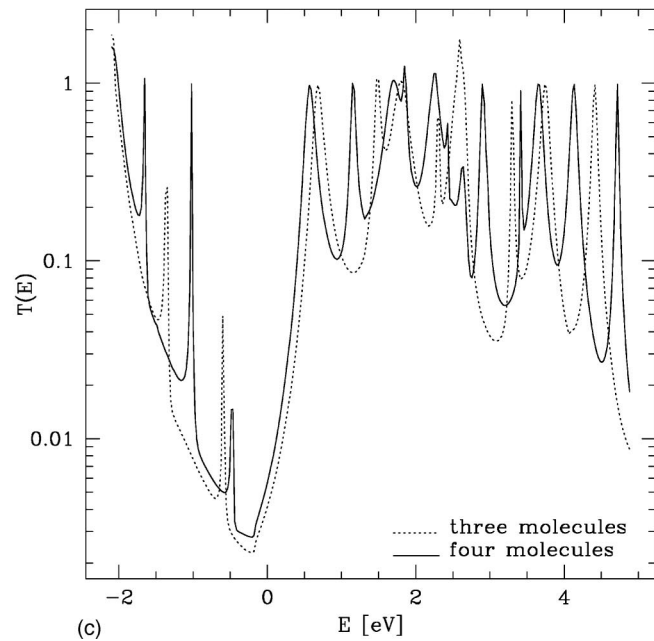
FIG. 6. (a) (Color online) Two, three, and four molecules with a shorter intermolecular distance. (b) The transmission functions for two and three molecules. (c) The transmission functions for three and four molecules. In contrast to all previous cases, the peaks are shifted with respect to each other and there are also additional peaks. These changes are due to the increase in intermolecular interaction, which alters the electronic levels.

molecules with two isocyanide groups a more or less random peak structure was observed in the *CV* characteristic.[9,14] In other devices, molecules with at least one thiol group are typically used. These show significantly less peak structure.

We therefore give the following interpretation: The thiol group is known to bind strongly to Au atoms. It is therefore likely that thiol-based monolayers stably adsorb to gold leads. Resulting periodic structures are then robust against distortions. The conductance of such structures is proportional to the corresponding single molecule conductance, i.e., the number of molecules involved changes the absolute value of the current only, not the peak structure.

The randomlike peak structure in devices made up of isocyanide based molecules suggests that there are some molecular clusters present in the monolayer. These clusters might occur, because the binding of an isocyanide group to Au is considerably weaker compared to that of a thiol group, and weaker binding results in a less robust periodic structure.
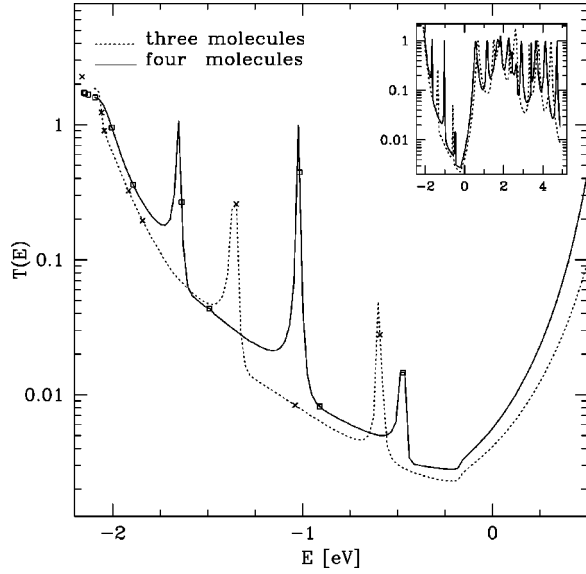
FIG. 7. Magnification of the transmission functions for three and four closely spaced molecules. Additionally the discrete energy levels of the system without leads are plotted as points along the transmission function. To each peak there belongs at least one discrete energy level. A detailed discussion is given in the main text. Inset: Transmission function (original scale) for three and four closely spaced molecules [identical to Fig. 6(c)].

APPENDIX A: CONNECTION BETWEEN EIGENVALUES AND CURRENT VALUES

For ease of notation we transform into the diagonal representation of the propagator P [Eq. (5)], i.e., $U^{-1}PU = \mathrm{diag}(\lambda^i)$. The current properties of each channel i can now be related to the corresponding eigenvalue λ_i. We start from Eq. (10):

$$\langle \psi | W_j | \phi \rangle = \langle \psi | W_{j+1} | \phi \rangle$$
$$= \lambda_1^* \lambda_2 \langle \psi | W_j | \phi \rangle.$$
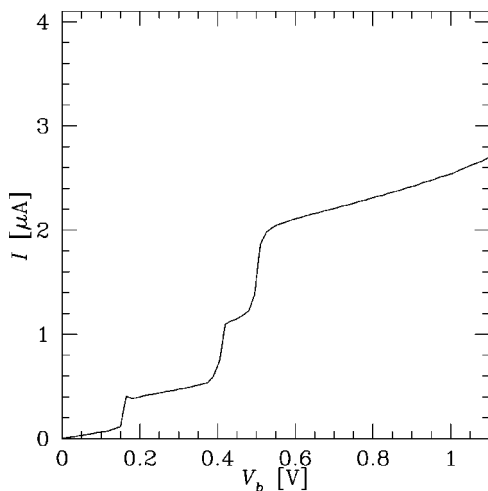
FIG. 8. *IV* calculation for a molecular region containing all three molecular clusters shown in Fig. 6(a). There are three distinct steps within the voltage range of 1 V.

Let us first consider $|\psi\rangle = |\phi\rangle$, i.e., $\lambda_1 = \lambda_2$, i.e., $\langle \psi | W_j | \phi \rangle = |\lambda| \langle \psi | W_j | \phi \rangle$. For each channel with eigenvalue $|\lambda| \neq 1$ one then must have $\langle \psi | W_j | \psi \rangle = 0$, i.e., this channel does not itself carry any current. This is consistent with our terminology of an evanescent wave. If, however, $|\lambda_i| = 1$, then $\langle \psi | W_j | \psi \rangle$ is purely imaginary, because W_j is an anti-Hermitian operator. We can therefore define the velocity of a propagating wave to be $v_i := \mathrm{Im}\langle \psi | W_j | \psi \rangle$.

Now we consider the case of two different solutions $|\psi\rangle \neq |\phi\rangle$ and define $v_{1,2} := \langle \psi | W_j | \phi \rangle$. If their eigenvalues do not satisfy $\lambda_1 \lambda_2^* = 1$, then the current between these two solutions is zero $v_{1,2} = 0$. So let us assume $\lambda_1 = 1/\lambda_2^*$. Because if $|\lambda_1| > 1$ then $|\lambda_2| < 1$, a current can flow between an evanescent left going wave and an evanescent right going wave. But if we restrict ourselves to solutions with finite amplitudes in a semi-infinite lead, then either the left or right going wave amplitude must be zero. Therefore evanescent waves do neither carry a current themselves nor do they exchange current with other channels, that is they do not at all contribute to the net current.

Finally we are left with the case $\lambda_1 = 1/\lambda_2^*$, with $|\lambda_1| = |\lambda_2| = 1$. This is equivalent to $\lambda_1 = \lambda_2$, i.e., the case of degenerate eigenvalues. Therefore propagating waves to degenerate eigenvalues may exchange current. However, within the degenerate eigenvalue subspace of P, we can perform an additional rotation, i.e., we can choose U such that the anti-Hermitian operator W is also diagonal with purely imaginary eigenvalues.

Summarizing we have shown that the transformation U diagonalizing the propagator P (i.e., $U^{-1}PU$) can be chosen such that the transformation $U^\dagger W U$ of the current operator is diagonal in the subspace of propagating waves with purely imaginary diagonal elements. All the other diagonal entries are zero and the only nonzero nondiagonal elements belong to evanescent waves in opposite directions.

APPENDIX B: CALCULATION OF THE SCATTERING MATRIX

The part of the Hamiltonian containing the molecular region and its coupling to the leads can be written as

$$(H - ES)|\psi\rangle = \begin{bmatrix} h_1 & M_1 & 0 & 0 & \tau_1^\dagger \\ 0 & 0 & h_2 & M_2 & \tau_2^\dagger \\ 0 & \tau_1 & 0 & \tau_2 & M_0 \end{bmatrix} |\psi\rangle = 0.$$

(B1)

(Using this order for the coefficients it is straightforward to extend all formulas to the general case of more than two leads.) The indices 1 and 2 indicate source and drain lead surface layers, while the index 0 is used for the molecular region. $\tau_{1,2}$ are the coupling matrices from source/drain to the molecules.

We now transform into the basis of incoming and outgoing channels [Eq. (12)], i.e., we apply

$$U = \begin{bmatrix} U^1 & 0 & 0 \\ 0 & U^2 & 0 \\ 0 & 0 & 1 \end{bmatrix} \quad \text{with} \quad U^i = \begin{bmatrix} U_>^i & U_<^i \\ U_>^i \Lambda_>^i & U_<^i \Lambda_<^i \end{bmatrix}$$

from the right to Eq. (B1):

$$(H - ES)U = \begin{bmatrix} A^1_> & A^1_< & 0 & 0 & \tau^\dagger_1 \\ 0 & 0 & A^2_> & A^2_< & \tau^\dagger_1 \\ B^1_> & B^1_< & B^2_> & B^2_< & M_0 \end{bmatrix}, \quad (B2)$$

with

$$A^i_\gtrless = h_i U^i_\gtrless + M_i U^i_\gtrless \Lambda^i_\gtrless ,$$

$$B^i_\gtrless = \tau_i U^i_\gtrless \Lambda^i_\gtrless .$$

The first and third columns act on the surface layer of the incoming channels, the second and fourth act on outgoing ones, while the fifth column, acting on the molecular region, remains unchanged.

The scattering matrix expresses the outgoing channel amplitudes in terms of the incoming ones. Therefore we split the matrix of Eq. (B2) into two parts, one containing the outgoing columns, the other one containing the incoming ones as well as the molecular column:

$$M_{out} := \begin{bmatrix} A^1_< & 0 & \tau^\dagger_1 \\ 0 & A^2_< & \tau^\dagger_2 \\ B^1_< & B^2_< & M_0 \end{bmatrix}, \quad M_{in} := \begin{bmatrix} A^1_> & 0 \\ 0 & A^2_> \\ B^1_> & B^2_> \end{bmatrix}.$$

The first matrix M_{out} is a square matrix and by inverting it, we obtain the scattering matrix

$$\mathcal{S} = - M^{-1}_{out} \cdot M_{in}. \quad (B3)$$

[1] S. Datta, W. Tian, S. Hong, R. Reifenberger, J.I. Henderson, and C.P. Kubiak, Phys. Rev. Lett. **79**, 2530 (1997).

[2] M. Magoga and C. Joachim, Phys. Rev. B **56**, 4722 (1997).

[3] E.G. Emberly and G. Kirczenow, Phys. Rev. B **64**, 235412 (2001).

[4] P.A. Derosa and J.M. Seminario, J. Phys. Chem. B **105**, 471 (2001).

[5] P. Damle, A.W. Ghosh, and S. Datta, Chem. Phys. **281**, 171 (2002).

[6] M. Brandbyge, J.L. Mozos, P. Ordejon, J. Taylor, and K. Stokbro, Phys. Rev. B **65**, 165401 (2002).

[7] P.S. Krstic, X.G. Zhang, and W.H. Butler, Phys. Rev. B **66**, 205319 (2002).

[8] A. Nitzan and M.A. Ratner, Science **300**, 1384 (2003).

[9] C.J.F. Dupraz, U. Beierlein, and J.P. Kotthaus, Chem. Phys. Chem. **4**, 1247 (2003).

[10] P. Sautet and C. Joachim, Chem. Phys. Lett. **185**, 23 (1989).

[11] J. Chen, M.A. Reed, A.M. Rawlett, and J.M. Tour, Science **286**, 1550 (1999).

[12] M.A. Reed, C. Zhou, C.J. Muller, T.P. Burgin, and J.M. Tour, Science **278**, 252 (1997).

[13] J. Reichert, R. Ochs, D. Beckmann, H.B. Weber, M. Mayor, and H.v. Löhneysen, Phys. Rev. Lett. **88**, 176804 (2002).

[14] J-O. Lee, G. Lientschnig, F. Wiertz, M. Struijk, R.A.J. Janssen, R. Egberink, D.N. Reinhoudt, P. Hadley, and C. Dekker, Nano Lett. **3**, 113 (2003).

[15] M.H. Hettler, W. Wenzel, M.R. Wegewijs, and H. Schoeller, Phys. Rev. Lett. **90**, 076805 (2003).

[16] M.J. Frisch *et al.*, Gaussian 98 (Revision A.7), Gaussian, Inc., Pittsburgh PA, 1998.

[17] S. Datta, *Electronic Transport in Mesoscopic Systems* (Cambridge University Press, Cambridge, UK, 1995).

[18] D.S. Fisher and P.A. Lee, Phys. Rev. B **23**, 6851 (1981).

[19] P. Sautet and C. Joachim, Phys. Rev. B **38**, 12238 (1988).

[20] D. Rosh, Ph.D. thesis, University of Cambridge, 1992.

[21] C. Zeng, B. Li, B. Wang, H. Wang, K. Wang, J. Yang, J.G. Hou, and Q. Zhu, J. Chem. Phys. **117**, 851 (2002).

[22] Y. Yourdshahyan and A.M. Rappe, J. Chem. Phys. **117**, 825 (2002).

[23] C.W. Bauschlicher, A. Ricca, N. Mingo, and J. Lawson, Chem. Phys. Lett. **372**, 723 (2003).